Published in final edited form as:
Nat Chem Biol. ; 8(3): 277–284. doi:10.1038/nchembio.773.

Menin-MLL Inhibitors Reverse Oncogenic Activity of MLL Fusion Proteins in Leukemia

Jolanta Grembecka[1,*], **Shihan He**[1], **Aibin Shi**[1], **Trupta Purohit**[1], **Andrew G. Muntean**[1], **Roderick J. Sorenson**[2], **Hollis D. Showalter**[2], **Marcelo Murai**[1], **Amalia Belcher**[3], **Thomas Hartley**[1], **Jay L. Hess**[1], and **Tomasz Cierpicki**[1,*]

[1]Department of Pathology, University of Michigan, Ann Arbor, MI, 48109, USA

[2]Department of Medicinal Chemistry, University of Michigan, Ann Arbor, MI, 48109, USA

[3]University of Virginia, Charlottesville, VA, 22908, USA

Summary

Translocations involving the *Mixed Lineage Leukemia* (*MLL*) gene result in human acute leukemias with very poor prognosis. The leukemogenic activity of MLL fusion proteins is critically dependent on their direct interaction with menin, a product of the *MEN1* gene. Here, we present the first small molecule inhibitors of the menin-MLL fusion protein interaction that specifically bind to menin with nanomolar affinities. These compounds effectively reverse MLL fusion protein-mediated leukemic transformation by downregulating the expression of target genes required for MLL fusion protein oncogenic activity. They also selectively block proliferation and induce both apoptosis and differentiation of leukemia cells harboring MLL translocations. Identification of these compounds provides a new tool for better understanding MLL-mediated leukemogenesis and represents a new approach for studying the role of menin as an oncogenic cofactor of MLL fusion proteins. Our findings also highlight a new therapeutic strategy for aggressive leukemias with MLL rearrangements.

Introduction

The *Mixed Lineage Leukemia* (*MLL*) gene is a common target of chromosomal translocations found in patients with acute myeloid leukemia (AML) and acute lymphoblastic leukemia (ALL) [1,2], affecting both children[3] and adults[4]. Fusion of *MLL* with one of over 50 different partner genes forms chimeric oncogenes encoding MLL fusion proteins, which preserve the N-terminal 1400 amino acid fragment of MLL fused to distinct protein partners[2,5–8]. MLL is required for the maintenance of *HOX* genes expression, which are important regulators of hematopoietic differentiation[9,10]. Disruption of *MLL* by translocation upregulates *HOX* expression, including *HOXA9*, *HOXA7* and the *HOX* cofactor *MEIS1*, which enhances proliferation and blocks hematopoietic differentiation,

*Correspondence: jolantag@umich.edu (J. G.) or tomaszc@umich.edu (T. C.), Phone: 734-615-9319, Fax 734-615-0688.

Author contributions

J.G. and T.C. initiated the project, lead the project team, designed experiments and analyzed results. S.H., T.P. and A.G.M. performed cellular assays. A.S., R.J.S., H.D.S. synthesized compounds. M.M. and T.H. expressed and purified proteins, run ITC and thermal shift assays. A.B. performed biochemical assays. J.L.H. designed experiments and analyzed results. J.G. and T.C. wrote the paper with input from all authors.

Competing Financial Interests Statement

The authors declare no competing financial interests.

Supplementary information, chemical compound and chemical probe information is available online at http://www.nature.com/naturechemicalbiology. Reprints and permissions information is available online at http://npg.nature.com/reprintsandpermissions/.

ultimately leading to acute leukemia[11–14]. MLL fusion proteins play a causative role in MLL-mediated leukemogenesis[15,16]. The presence of *MLL* translocations in leukemia patients is generally associated with a very poor prognosis[6,17,18], emphasizing the pressing need for developing more effective therapies for the treatment of MLL leukemias.

The leukemogenic activity of MLL fusion proteins is critically dependent on their direct interaction with menin[19–21], a protein encoded by the *Multiple Endocrine Neoplasia 1* (*MEN 1*) gene[22]. Menin is a tumor suppressor protein which directly controls cell growth in endocrine organs[23]. Menin is also a highly specific partner of MLL, and an essential component of the MLL SET1-like histone methyl transferase complex[24,25]. Association of menin with MLL fusion proteins upregulates expression of target genes, such as *HOXA9* and *MEIS1*, and is critical for oncogenic transformation induced by MLL fusion oncoproteins[19,21]. Myeloid cells transformed with oncogenic MLL-AF9 require menin for efficient proliferation[21]. Loss of menin relieves the differentiation block induced by MLL fusion proteins in transformed leukemic blasts[19]. Mutations within the N-terminus of MLL fusion proteins that block association with menin abrogate the development of acute leukemia in mice[19,20]. These findings demonstrate that menin functions as an essential oncogenic co-factor of MLL fusion proteins, and implies that the menin-MLL interaction represents a valuable target for molecular therapy[19–21]. A small molecule that specifically binds to menin and inhibits the menin-MLL interaction would be a valuable tool to study the molecular mechanism of MLL-mediated leukemogenesis and might lay a foundation for novel targeted therapy for MLL leukemias.

We have recently characterized the molecular basis of the menin interaction with the N-terminal fragment of MLL[26]. The major objective of the studies presented here was to develop small molecule inhibitors of the protein-protein interaction between menin and MLL fusion proteins and evaluate if such compounds are capable of blocking the leukemogenic activity of MLL fusion proteins. By applying high throughput screening (HTS) we identified small molecule inhibitors of the menin-MLL interaction, which we then optimized by medicinal chemistry to develop inhibitors with nanomolar affinities. These compounds, which represent the first reported small molecule inhibitors of the menin-MLL interaction, reverse the leukemogenic activity of MLL fusion proteins by downregulating the expression of *HOXA9* and *MEIS1*. They also block proliferation and induce both apoptosis and differentiation of MLL leukemia cells. Our results demonstrate the utility of menin-MLL inhibitors as chemical tools to study the mechanism of leukemogenesis mediated by MLL fusion proteins. Furthermore, our work strongly supports the rationale of targeting the menin-MLL interaction with small molecules as a novel therapeutic approach for acute leukemias associated with *MLL* translocations.

Results

Identification of menin-MLL inhibitors

We employed HTS to identify initial lead compounds targeting menin and inhibiting the menin-MLL interaction. We screened a collection of 49,000 small molecules using a fluorescence polarization (FP) assay with a fluorescein labeled MLL derived peptide comprising the high affinity menin binding motif (MBM1)[26], (Supplementary Methods and Supplementary Results, Supplementary Table 1). A step-wise procedure, including two FP assays with fluorescein and Texas Red labeled MBM1 followed by NMR experiments to validate binding of compounds to menin, was applied to identify menin-MLL inhibitors. The most potent compound identified by HTS, **MI-1** (**1**), which belongs to the thienopyrimidine class, reversibly inhibited the menin-MLL interaction with an IC_{50} value of 1.9 μM (Fig. 1a and Supplementary Fig. 1a). We have also identified two other compounds belonging to the

thienopyrimidine class, but they were 20–40 fold weaker than **MI-1** (Supplementary Fig. 1b).

To validate that **MI-1** directly binds to menin and competes with MLL, we employed Saturation Transfer Difference (STD) NMR experiments[27] (Supplementary Methods). A strong STD effect was observed for **MI-1**, indicative of its direct binding to menin (Fig. 1b). We then employed a competition STD experiment to assess whether **MI-1** competes with MLL for binding to menin. Indeed, addition of the MBM1 peptide to the menin-**MI-1** complex significantly decreased the STD effect for **MI-1** in a dose dependent manner (Fig. 1b). This demonstrates that binding of **MI-1** and MLL to menin is mutually exclusive and confirms the reversible and specific binding of **MI-1** to menin.

Development of potent menin-MLL inhibitors

We explored both commercial and synthesized compounds to develop the structure-activity relationship (SAR) for analogues of the **MI-1** lead compound with modifications at R1 and R2 positions (Fig. 1c and Supplementary Tables 2 and 3). We introduced several heterocyclic rings at R2 and the dimethyl-thiazoline group represented the best substituent (Fig. 1c and Supplementary Tables 2 and 3). Assessment of diverse hydrophobic groups at R1 led to the development of several compounds with IC_{50} values in the nanomolar range, including **MI-2** (**2**) (IC_{50} = 446 ± 28 nM) and **MI-3** (**3**) (IC_{50} = 648 ± 25 nM) (Fig. 1a, Supplementary Fig. 1c and Supplementary Scheme 1). We validated the specific binding of these compounds to menin by competition STD NMR experiments (Supplementary Fig. 2a,b). The n-propyl represented an optimal substituent at R1 while a larger hydrophobic group or branched aliphatic chains were not well tolerated (Supplementary Table 3). As a negative control compound, we selected a compound sharing the same molecular scaffold and similar functional groups, **MI-nc** (**4**), (Fig. 1a and Supplementary Scheme 2), which showed very weak *in vitro* inhibition of the menin-MLL interaction (IC_{50} = 193 μM). In order to assess the binding affinities of the most potent compounds, we employed Isothermal Titration Calorimetry (ITC) (Supplementary Methods). The dissociation constants measured for the menin-MLL inhibitors were at the nanomolar level, K_d = 158 nM for **MI-2** (Fig. 1d), and K_d = 201 nM for **MI-3** (Supplementary Fig. 2c). Importantly, the stoichiometry of binding of both compounds to menin was 1:1, which further supports their specific binding to the protein.

We have recently determined the crystal structure of a menin homolog from *Nematostella vectensis* and mapped the MLL binding site to a large central cavity on menin[28]. To assess whether menin inhibitors interact with the same pocket were MLL binds, we employed the thermal shift assay (Supplementary Methods) and tested binding of menin inhibitors to the wild-type menin as well as to two point mutants (M278K and Y323K) which lack binding to MLL[28]. As expected, we clearly observed binding of **MI-2** and **MI-3** to the wild-type menin (Supplementary Fig. 3). In contrast, we detected no binding of **MI-2** and **MI-3** to M278K and Y323K menin mutants (Supplementary Table 4). These data further emphasize the specificity of compound interaction with the protein and also map the compound binding site to the MLL binding site on menin.

Inhibition of the menin-MLL fusion interaction in cells

To test if the most potent compounds disrupt the menin-MLL-AF9 interaction in mammalian cells, we performed co-immunoprecipitation (co-IP) experiments in HEK293 cells transfected with Flag-MLL-AF9 (Supplementary Methods, Fig. 1e and Supplementary Figure 4). Expression of endogenous menin was validated by Western blot. Menin co-IPs with MLL-AF9 in DMSO treated sample (Fig. 1e). Treatment with **MI-2** and **MI-3**, however, very efficiently disrupted the menin-MLL-AF9 complex without affecting the

expression level of menin and MLL-AF9 (Fig. 1e). In contrast, we observed no effect in the co-IP experiment for the negative control compound **MI-nc** (Fig. 1e). These data demonstrate that **MI-2** and **MI-3** can access the protein target and very effectively inhibit the menin-MLL-AF9 interaction in human cells.

Menin-MLL inhibitors induce cell growth arrest

Disruption of the menin-MLL fusion protein interaction should result in cell growth arrest[19,20]. To determine whether such an effect can be achieved upon treatment with the menin-MLL inhibitors, we tested **MI-2** and **MI-3** in mouse bone marrow cells (BMC) transduced with MLL-AF9 and MLL-ENL (Supplementary Fig. 5a). As a control, we used BMC transduced with the E2A-HLF oncogene, which is not dependent on *Hoxa9* for transformation. Cell growth inhibition was assessed using the MTT cell viability assay[29] (Supplementary Methods). The menin-MLL inhibitors very effectively blocked proliferation of MLL-AF9 and MLL-ENL transduced BMC, with GI_{50} values of about 5 μM for **MI-2** and **MI-3** (Fig. 2a and Supplementary Fig. 5b). Substantial inhibition of cell proliferation was also reflected in growth curves (Fig. 2b and Supplementary Fig. 5c). In contrast, **MI-nc**, which is a very weak inhibitor of the menin-MLL interaction, showed a very little effect on proliferation of MLL fusion transduced BMC (Fig. 2a and 2b). Because **MI-nc** is chemically very similar to the active compounds (Fig. 1a), the lack of activity of this compound serves as evidence that the observed effects are due to specific targeting of the menin-MLL fusion protein interaction rather than off-target effects. Furthermore, **MI-2** and **MI-3** showed only a small effect on the cell growth of E2A-HLF transduced BMC (GI_{50} > 50 μM, Fig. 2a and Supplementary Fig. 5b), which may be due to inhibition of the menin interaction with wild-type MLL. Overall, these results demonstrate high specificity of the menin-MLL inhibitors towards MLL fusion protein transformed cells.

Menin-MLL inhibitors block transformation by MLL fusions

To assess the effect of menin-MLL inhibitors on transforming potential of MLL fusion proteins, we utilized colony formation assays with MLL-AF9 transformed BMC. The E2A-HLF transduced BMC served as a negative control. **MI-2** and **MI-3** substantially reduced colony formation in MLL-AF9 transformed cells (Fig. 2c and Supplementary Fig. 5d). After replating and culturing for an additional 7 days, we observed a greater inhibition of colony formation with **MI-2** and **MI-3** (Supplementary Fig. 5e). In contrast, we detected a very weak effect on colony formation for the **MI-nc** (Fig. 2c). Importantly, the morphology and size of the colonies were also dramatically different upon treatment with **MI-2** and **MI-3** (Fig. 2d and Supplementary Fig. 5f). Colonies for DMSO or **MI-nc** treated cells were large and displayed a dense, compact, blast-like morphology, indicative of transformation[30]. In contrast, treatment with **MI-2** and **MI-3** resulted in much smaller, diffuse colonies, indicative of differentiation (Fig. 2d and Supplementary Fig. 5f). Very similar effects were observed upon acute loss of menin[19] and after overexpression of a dominant negative fragment of MLL[20]. Importantly, we observed only a limited effect of **MI-2** on the number, size and morphology of colonies formed with E2A-HLF transformed BMC (Fig. 2c and Supplementary Fig. 5g), with no statistically significant difference between treatment with **MI-2** and **MI-nc**. Overall, these data demonstrate that **MI-2** and **MI-3** substantially and specifically reduce the immortalization potential of cells transformed with MLL fusion oncoproteins.

Menin-MLL inhibitors induce hematopoietic differentiation

Myeloid blasts transformed by MLL oncoproteins are critically dependent on interaction with menin to effectively maintain their undifferentiated state [19,20]. Therefore, we tested whether **MI-2** and **MI-3** can induce differentiation in MLL fusion protein transformed cells

(Supplementary Methods). Indeed, we observed that the MLL-AF9 transformed BMC that remained viable after 7 days of treatment with **MI-2** and **MI-3** showed substantial changes in morphology, indicative of monocytic differentiation, as evidenced by increased cell size, lower nuclear to cytoplasmic ratio and highly vacuolated cytoplasm (Fig. 3a and Supplementary Fig. 6a). By 10 days, the effect was more dramatic as a majority of the cells treated with **MI-2** and **MI-3** differentiated into macrophages (Fig. 3a and Supplementary Fig. 6b). In contrast, cells treated with DMSO or **MI-nc** failed to differentiate and maintained a blast-like morphology (Fig. 3a and Supplementary Fig. 6b). Likewise, we also observed differentiation in MLL-ENL transformed BMC treated with **MI-2** and **MI-3**, while no effect was detected after treatment with **MI-nc** (Supplementary Fig. 6b). Furthermore, the E2A-HLF transformed BMC did not differentiate under treatment with **MI-2**, **MI-3** or **MI-nc** (Supplementary Fig. 6c), validating the specificity of the menin-MLL inhibitors for the MLL fusion protein transformed cells.

We also monitored differentiation of MLL-AF9 transformed BMC by detecting the expression level of CD11b, a differentiation marker of myeloid cells. Consistent with the change in cell morphology, the expression of CD11b was substantially increased on MLL-AF9 transformed BMC after 7 days of treatment with **MI-2** and **MI-3** (Fig. 3b and Supplementary Fig. 7a). No increase in CD11b expression was detected for **MI-nc**, (Fig. 3b). Collectively, these findings reveal that inhibition of the menin-MLL fusion protein interaction by small molecule inhibitors relieves the differentiation block in MLL fusion protein transformed leukemic blasts, closely recapitulating the effects observed after acute loss of menin in leukemic cells[19].

Menin-MLL inhibitors downregulate MLL fusion target genes

Interaction between menin and MLL fusion proteins is required for the maintenance of *Hox* gene expression in MLL fusion protein transformed cells[19,20]. Therefore, we tested whether inhibition of the menin-MLL fusion protein interaction by small molecules leads to downregulation of target genes important for transformation. The expression level of *Hoxa9* and *Meis1* measured by quantitative RT-PCR was substantially reduced in MLL-AF9 transduced BMC, with more than an 80% decrease after 6 days of treatment with 25 μM and 12.5 μM of **MI-2** (Fig. 3c). We also observed a similar effect in cells transformed with MLL-ENL (Supplementary Fig. 7b). These results show that disruption of the menin-MLL fusion protein interaction by small molecules effectively downregulates expression of target genes required for leukemogenic activity of MLL fusion proteins. These data are in agreement with the results obtained after acute loss of menin[19], as well as, upon expression of the dominant negative MLL fragment[20].

MI-2 reduces menin-MLL-AF9 occupancy on the Hoxa9 locus

Menin associates with MLL oncoproteins on *Hox* gene promoters[19,20]. To establish whether menin-MLL inhibitors deplete menin at the *Hoxa9* locus, we performed chromatin immunoprecipitation (ChIP) assays in MLL-AF9 transduced BMC (Supplementary Methods). Using the anti-menin and anti-AF9 antibody, which recognizes the C-terminus of AF9 retained in the fusion protein[31], we demonstrated that both menin and MLL-AF9 were present at the *Hoxa9* promoter in the control samples treated with DMSO (Fig. 3d). As expected, treatment with **MI-2** decreased binding of menin and MLL-AF9 to the *Hoxa9* locus (Fig. 3d). This remains in agreement with the previous studies emphasizing cooperative localization of menin and MLL fusion proteins to the *Hoxa9* locus[19,20,31]. Treatment with **MI-2** also resulted in elevated levels of histone H3 reflecting an increase in chromatin condensation after reduction of MLL-AF9 and menin occupancy on the *Hoxa9* locus (Fig. 3e). This was also accompanied by a decrease in H3K4 tri-methylation and H3K79 di-methylation (Fig. 3e), consistent with a decrease in transcriptional activity at the

Hoxa9 locus after treatment with **MI-2**. Importantly, our results closely recapitulate the epigenetic changes observed upon excision of *Men1* in MLL-AF9 transformed cells[31].

Effect of menin-MLL inhibitors in human leukemia cells

Next, we have tested **MI-2** and **MI-3** in a panel of human MLL leukemia cell lines harboring different MLL translocations. Both compounds showed an effective and dose-dependent growth inhibition of several cell lines with different MLL translocations (Fig. 4a and Supplementary Figure 8a). Treatment with **MI-2** resulted in GI_{50} values below 10 μM in MV4;11 (harboring MLL-AF4; GI_{50} = 9.5 μM), KOPN-8 (MLL-ENL; GI_{50} = 7.2 μM) and ML-2 (MLL-AF6; GI_{50} = 8.7 μM), and in MonoMac6 (MLL-AF9; GI_{50} = 18 μM) (Fig. 4a and Supplementary Fig. 8a). Very similar results were obtained for **MI-3** (Fig. 4a). A pronounced effect of **MI-2** and **MI-3** on cell growth was also seen in other MLL leukemia cells (Supplementary Fig. 8a). In contrast, **MI-nc** displayed a significantly weaker effect on proliferation of MLL leukemia cells (Fig. 4a and Supplementary Fig. 8a). The small effect observed upon treatment of MV4;11 and ML-2 cells with **MI-nc** may result from higher sensitivity of these cells to the menin-MLL inhibitors or a small cytotoxic effect of this compound when used at higher doses.

To assess specificity, we assayed the effects of **MI-2** and **MI-3** on the growth of several human acute leukemia cell lines lacking MLL fusions and expressing a low level of *HOXA9*, such as Kasumi-1, ME-1, HAL-01 and REH[32,33]. Both compounds, as well as **MI-nc**, showed a very limited effect on proliferation of these cells (Fig. 4a and Supplementary Fig. 8b). Interestingly, we detected some effect of **MI-2** and **MI-3**, but less pronounced for **MI-nc,** on the cell growth of leukemic cells lacking MLL fusions but expressing high or moderate levels of *HOXA (HOXA9*, *HOXA7*, *HOXA10)* and/or *MEIS1*, such as U937, HL-60 and K562 cell lines[33–35], Supplementary Fig. 8c. This effect most likely results from inhibition of the menin interaction with wild type MLL, suggesting that these compounds could potentially be utilized in other acute leukemias with elevated level of *HOXA* genes[32,36,37]. Together, these results demonstrate that **MI-2** and **MI-3** can selectivity target MLL leukemia cells resulting in inhibition of cell growth, emphasizing that these effects should result from on-target effects of these compounds.

We assessed the effect of compounds on apoptosis in two MLL leukemia cell lines, MV4;11 and MonoMac6, by flow cytometry analysis of Annexin V/Propiduim Iodide (PI) stained cells. Treatment with **MI-2** and **MI-3** for 48h resulted in a substantial, and dose-dependent increase in Annexin V (+) and Annexin V/PI (+)/(+) cells (Fig. 4b and Supplementary Fig. 9a), demonstrating an increase in the number of cells undergoing apoptosis. On the contrary, we did not observe such effect for **MI-nc** (Fig. 4b). Increased incubation time with **MI-2** and **MI-3** resulted in more pronounced apoptosis (Supplementary Fig. 9b). The increased apoptosis seen with the menin-MLL inhibitors is consistent with the data reported for the siRNA treatment of the RS4;11 leukemia cells harboring the MLL-AF4 translocation[38]. In contrast, we detected very limited or no apoptosis in the non-MLL leukemia cells after treatment with **MI-2** (Supplementary Fig. 9c), further demonstrating specificity of this compound towards MLL leukemia cells.

We also assessed the effect of menin-MLL inhibitors on cell cycle progression (Supplementary Methods) and observed a consistent increase in the number of cells in G0/G1 phase following treatment of MV4;11 leukemia cells with **MI-2** (Fig. 4c,d). Concomitantly, we detected a significant decrease in the population of cells in S and G phases of the cell cycle. These data are consistent with the G0/G1 cell cycle arrest observed after acute loss of menin in the MLL-ENL transformed bone marrow cells[19]. In contrast, we

observed no significant changes in cell cycle for the negative control compound **MI-nc** (Fig. 4c,d).

Differentiation and HOX downregulation in leukemia cells

We determined the effect of the menin-MLL inhibitors on differentiation of human MLL leukemia cells harboring different MLL translocations, and detected a marked morphology change after treatment with **MI-2** and **MI-3** indicating that these cells undergo hematopoietic differentiation (Fig. 4e and Supplementary Figs. 10–13). Cell morphology did not change under treatment with **MI-nc** (Fig. 4e and Supplementary Figs. 10–13). Furthermore, we detected a substantial increase in CD11b positive cells upon 6 days of treatment of THP-1 cells with **MI-2** and **MI-3** (Fig. 4f and Supplementary Fig. 10b,c). In contrast, treatment with **MI-nc** did not result in an increase of CD11b expression (Fig. 4f). Together, these results demonstrate that inhibition of the menin-MLL fusion protein interaction by **MI-2** and **MI-3** relieves differentiation block induced by MLL fusion proteins in human leukemia cells.

HOX cluster genes, particularly *HOXA9* and *HOXA7*, and the *HOX* cofactor *MEIS1,* are highly expressed in MLL-associated leukemias[11,12,39]. We found that treatment of THP-1 cells with **MI-2** and **MI-3** resulted in substantially reduced expression of *HOXA9* and *MEIS1* (Fig. 4g). In addition, we observed downregulation of other genes dependent on the menin-MLL interaction (*HOXA7*, *HOXA10* and $p27^{Kip1}$)[19,40] (Supplementary Fig. 14). These results demonstrate that small-molecule inhibitors of the menin-MLL fusion protein interaction effectively downregulate expression of downstream targets of MLL-fusion proteins required for their leukemogenicity in human leukemia cells. These findings are in agreement with the data reported for the menin conditional knock-out[19] and upon expression of a dominant negative MLL fragment[20].

Discussion

Menin plays a critical role as an oncogenic cofactor of MLL fusion proteins, and the menin-MLL interaction was validated as a potential therapeutic target in acute leukemias with MLL rearrangements [19,20]. Inhibition of the menin-MLL fusion protein interaction by small molecules could represent a novel therapeutic strategy for leukemia patients with MLL translocations. Here we report development of small molecules, **MI-2** and **MI-3**, that specifically bind to menin with nanomolar affinities and are potent and reversible inhibitors of the menin-MLL interaction *in vitro* and in human cells. The *in vitro* inhibition of the menin-MLL interaction and the cellular response to treatment with these compounds, such as inhibition of proliferation, apoptosis and differentiation of MLL fusion protein transformed cells, are well correlated. Downregulation of *HOXA9* and *MEIS1* expression, inhibition of transforming properties of MLL fusion proteins, and reduced occupancy of the menin-MLL fusion protein complex on the *Hoxa9* promoter induced by these compounds strongly supports specificity in their mechanism of action. These results imply that the cellular activities of **MI-2** and **MI-3** are through on-target effects. Overall, our results demonstrate for the first time that development of small-molecule inhibitors targeting the menin-MLL interaction is feasible and that such compounds are capable of reversing the leukemogenic activity of MLL fusion proteins. The effects observed upon treatment with these compounds closely recapitulate the effects of disruption of the menin-MLL fusion protein interaction achieved by excision of the menin binding motif from the N-terminus of MLL-GAS7 and MLL-ENL fusion proteins[19]. They also recapitulate the effects observed in MLL fusion protein transduced bone marrow progenitor cells following acute loss of menin[19] or the expression of a dominant negative N-terminal fragment of MLL[20].

MI-2 and **MI-3** are valuable chemical probes that can be used to study the biology and mechanism of MLL-fusion protein mediated leukemogenesis and to further validate the role of menin as an oncogenic co-factor of MLL fusion proteins. These compounds also represent a valuable pharmacophore that can be applied to address the potential therapeutic benefit of inhibiting the menin-MLL interaction and might result in development of therapeutically useful compounds for leukemia patients with rearrangements of the *MLL* gene.

The menin binding motif is located at the N-terminus of MLL[19,20,26] and is preserved in wild-type MLL and in all MLL fusion proteins. Therefore, targeting the menin-MLL interaction represents a general approach to inhibit the leukemogenic activity of all MLL fusion proteins regardless of the fusion partner. Due to inhibition of the menin-MLL wild-type interaction, **MI-2** and **MI-3** may also serve as valuable chemical probes to improve our understanding of menin's precise role in complex with MLL during hematopoiesis and in transcriptional regulation. Furthermore, the MLL-AF9 fusion protein requires the expression of wild-type MLL to induce and maintain leukemogenic transformation[31]. Therefore, simultaneous targeting of the menin-MLL and menin-MLL fusion protein interactions by small-molecule inhibitors reported here could effectively block oncogenesis by MLL fusion proteins. Future efforts will be undertaken to improve the therapeutic potential of the compounds identified in this study with the goal of developing targeted therapy for acute leukemia patients with translocations of the *MLL* gene and possibly other acute leukemias with upregulated *HOX* genes [32,36,37]. These compounds possess desirable properties, such as high target potency, selectivity, low molecular weight (below 400 Da), synthetic accessibility and utility in experimental biology. This establishes the plausibility of developing both drug-like derivatives for therapeutic application and chemical probes for further understanding the biology and oncogenic activity of MLL fusion proteins.

Methods

Protein expression

The expression and purification of menin was done as described previously[26].

High Throughput Screening

FITC-MBM1 at 15 nM and menin at 150 nM in the FP buffer (Supplementary Table 1) were mixed and incubated for 1h in the dark at room temperature. A collection of 49,000 compounds from the Center for Chemical Genomics, University of Michigan, was used for HTS. For point screening, the 0.2 μL of each compound (20 μM final concentration, 1% DMSO) was added to 20 μL of the aliquot of the protein-peptide mixture and incubated on 384-well plates in the dark at room temperature for 1h. In confirmation screening, the serial dilution plates with compounds in DMSO were prepared and used to titrate the menin-FITC-MBM1 complex. Change in fluorescence polarization was monitored at 525 nm after excitations at 495 nm using the PHERAstar microplate reader (BMG) and applied to determine IC_{50} values with the Origin 7.0 program.

Cell lines and cell culture

HEK 293 cells were cultured in Dulbecco's modified Eagle's medium, DMEM, (Invitrogen) supplemented with 10% fetal bovine serum, FBS, (Invitrogen), and 1× non-essential amino acids, NEAA, (Invitrogen). KOPN-8, ML-2, Kasumi-1 and ME-1 cells were cultured in Roswell Park Memorial Institute (RPMI-1640) medium (Invitrogen) supplemented with 10% FBS. MV4;11 and THP-1 cells were cultured in RPMI-1640 medium with 10% FBS, 1% penicillin/streptomycin and NEAA. MonoMac-6 cells were cultured in RPMI-1640 medium with 15% FBS, human insulin, 1% penicillin/streptomycin (Invitrogen) and NEAA.

Mouse bone marrow cells

MLL-AF9, MLL-ENL and E2A-HLF transduced mouse bone marrow cells were prepared as described previously [41]. These cells were cultured in IMDM media supplemented with 15% FBS, 1% penicillin/streptomycine and IL-3.

Vector construction

The expression vector for Flag-MLL-AF9 was prepared as described previously[41].

Chromatin immunoprecipitation assay (ChiP)

ChiP was performed in MLL-AF9 transduced BMC treated with **MI-2** or DMSO using the procedure described previously [42]. Primary antibodies specific for AF9, Menin (Bethyl), histone H3, H3K4 trimethylation, and H3K79 dimethylation (Abcam) were used, see Supplementary Methods for details.

Annexin V/PI assay of inhibitor effects on apoptosis

5×10^5 cells/ml were plated in 12-well plates (1ml/well) and treated with compounds (0.25% final concentration of DMSO for each condition) or 0.25% DMSO control and incubated for 48h at 37 °C in a 5% CO_2 incubator. After incubation, 1.5×10^5 cells were harvested and resuspended in 100 μl 1× Annexin V binding buffer from the Annexin V-FITC Apoptosis kit (BD Biosciences Pharmingen), incubated with 4 μl of AnnexinV-FITC and 6 μl of Propidium iodide (Sigma-Aldrich) at room temperature in the dark for 10 minutes and analyzed by flow cytometry on a LSR II instrument. Data analysis was performed using WinList software. The experiments were performed three times in triplicates with calculation of mean and standard deviation for each condition.

Inhibitor effects on expression of CD11b

THP-1 cells or MLL-AF9 transduced bone marrow cells were plated in 12-well plates at initial concentration of 5×10^5 cells/ml and treated with compounds or 0.25% DMSO. Media were changed every 48h with viable cell concentration restored to 5×10^5 cells/ml and compounds resupplied. Six days after the experiment was set-up, the 1.5×10^5 cells were harvested and washed with FACS buffer (PBS, 1% FBS, 0.1% NaN_3). Cells were resuspended in 100 μl FACS buffer and incubated with 2 μl Pacific Blue mouse anti-human CD11b antibody (BD Biosciences) or 1 μl Pacific Blue rat anti-mouse CD11b antibody (BioLegend) at 4°C for 30 min. Cells were then washed, resuspended in 100 μl Annexin V binding buffer, and incubated with 4 μl Annexin V-FITC (BD Biosciences) and 6 μl Propidium iodide (1mg/ml, Sigma-Aldrich) at room temperature for 10 min before being analyzed by flow cytometry.

Colony formation assay

The MLL-AF9 and E2A-HLF transduced murine BMC were plated in 12-well plates at the concentration of 5×10^3 cells/ml with 1 ml methylcellulose medium M3234 (StemCell Technologies) containing 20% IMDM medium, 1% penicillin/streptomycin, IL-3 and 0.25% DMSO or compounds. 6 days later colonies were stained with 100 μl iodonitrotetrazolium chloride (Sigma-Aldrich) at final concentration of 1mg/ml, incubated at 37°C for 30 min and counted. To replate for the 2nd round, colonies were counted at day 6 without staining and cells were washed out by 1×PBS buffer and resuspended in IMDM medium containing 15% FBS, 1% penicillin/streptomycin and IL-3. 5×10^3 cells were plated in 12-well plates with 1ml methycellulose medium M3234 (StemCell Technologies, Inc.) containing 20% IMDM medium, 1% penicillin/streptomycin, IL-3 and 0.25% DMSO or compounds. 6 days later colonies were stained and counted.

Real-Time PCR

Total RNA was extracted from cells using RNeasy mini kit (Qiagen). 100 ng – 1000 ng of total RNA was reverse transcribed using High Capacity cDNA Reverse Transcription Kit (Applied Biosystems) according to the manufacturer's protocol. Real-time PCR was performed using the ABI Prism 7700 sequence detection system. Taqman Gene Expression Master Mix and Taqman Gene Expression Assays for mouse *Hoxa9* (Mm00439364_m1), *Meis1* (Mm00487664_m1), *β-Actin* (4352933), human *HOXA9* (Hs00365956_m1), *MEIS1* (Hs00180020_m1) and 18S RNA (Hs99999901_s1) were purchased from Applied Biosystems. Relative quantification of each gene transcript was carried out using the comparative C_t method as described in the Applied Biosystems User Bulletin No. 2.

Statistical analysis

Mean values and standard deviations were calculated to estimate the degree of data variation, as specified for each experiment in Figure legend. GraphPad Prism software was used for statistical analysis. Two-way ANOVA analysis was applied to calculate the statistical significance of the data (P values).

Supplementary Material

Refer to Web version on PubMed Central for supplementary material.

Acknowledgments

This work was supported by grants from the Leukemia and Lymphoma Society (TRP grant 6070-09 to J.G. and LLS SCOR grant to J.L.H.), NIH R01 (1R01 CA-160467-01 to J.G.), Cancer Center (University of Virginia to J.G. and T.C.), Children's Leukemia Research Association (to J.G.), American Cancer Society (RSG-11-082-01-DMC to TC) and startup funds to J.G. and T.C. provided by the Department of Pathology (University of Michigan). The authors greatly appreciate support from Dr. John Bushweller (University of Virginia) for providing the research environment for carrying out part of these studies. We are grateful to Martha Larsen from the Center for Chemical Genomics, University of Michigan, for technical expertise during HTS. We would like to thank Jiaying Tan (University of Michigan) for discussion of experimental procedures and Dr. Ronald Craig from the Department of Pathology (University of Michigan) for technical support with flow cytometry experiments.

References

1. Pui CH, et al. Outcome of treatment in childhood acute lymphoblastic leukaemia with rearrangements of the 11q23 chromosomal region. Lancet. 2002; 359:1909–15. [PubMed: 12057554]
2. Liu H, Cheng EH, Hsieh JJ. MLL fusions: pathways to leukemia. Cancer Biol Ther. 2009; 8:1204–11. [PubMed: 19729989]
3. Sorensen PH, et al. Molecular rearrangements of the MLL gene are present in most cases of infant acute myeloid leukemia and are strongly correlated with monocytic or myelomonocytic phenotypes. J Clin Invest. 1994; 93:429–37. [PubMed: 8282816]
4. Cox MC, et al. Chromosomal aberration of the 11q23 locus in acute leukemia and frequency of MLL gene translocation: results in 378 adult patients. Am J Clin Pathol. 2004; 122:298–306. [PubMed: 15323147]
5. Hess JL. MLL: a histone methyltransferase disrupted in leukemia. Trends Mol Med. 2004; 10:500–7. [PubMed: 15464450]
6. Popovic R, Zeleznik-Le NJ. MLL: how complex does it get? J Cell Biochem. 2005; 95:234–42. [PubMed: 15779005]
7. Krivtsov AV, Armstrong SA. MLL translocations, histone modifications and leukaemia stem-cell development. Nat Rev Cancer. 2007; 7:823–33. [PubMed: 17957188]
8. Slany RK. The molecular biology of mixed lineage leukemia. Haematologica. 2009; 94:984–93. [PubMed: 19535349]

9. Hess JL, Yu BD, Li B, Hanson R, Korsmeyer SJ. Defects in yolk sac hematopoiesis in Mll-null embryos. Blood. 1997; 90:1799–806. [PubMed: 9292512]
10. Lawrence HJ, et al. Mice bearing a targeted interruption of the homeobox gene HOXA9 have defects in myeloid, erythroid, and lymphoid hematopoiesis. Blood. 1997; 89:1922–30. [PubMed: 9058712]
11. Rozovskaia T, et al. Upregulation of Meis1 and HoxA9 in acute lymphocytic leukemias with the t(4:11) abnormality. Oncogene. 2001; 20:874–8. [PubMed: 11314021]
12. Ayton PM, Cleary ML. Transformation of myeloid progenitors by MLL oncoproteins is dependent on Hoxa7 and Hoxa9. Genes Dev. 2003; 17:2298–307. [PubMed: 12952893]
13. Zeisig BB, et al. Hoxa9 and Meis1 are key targets for MLL-ENL-mediated cellular immortalization. Mol Cell Biol. 2004; 24:617–28. [PubMed: 14701735]
14. Wong P, Iwasaki M, Somervaille TC, So CW, Cleary ML. Meis1 is an essential and rate-limiting regulator of MLL leukemia stem cell potential. Genes Dev. 2007; 21:2762–74. [PubMed: 17942707]
15. Argiropoulos B, Humphries RK. Hox genes in hematopoiesis and leukemogenesis. Oncogene. 2007; 26:6766–76. [PubMed: 17934484]
16. Rice KL, Licht JD. HOX deregulation in acute myeloid leukemia. J Clin Invest. 2007; 117:865–8. [PubMed: 17404613]
17. Ernst P, Wang J, Korsmeyer SJ. The role of MLL in hematopoiesis and leukemia. Curr Opin Hematol. 2002; 9:282–7. [PubMed: 12042701]
18. Slany RK. When epigenetics kills: MLL fusion proteins in leukemia. Hematol Oncol. 2005; 23:1–9. [PubMed: 16118769]
19. Yokoyama A, et al. The menin tumor suppressor protein is an essential oncogenic cofactor for MLL-associated leukemogenesis. Cell. 2005; 123:207–18. [PubMed: 16239140]
20. Caslini C, et al. Interaction of MLL amino terminal sequences with menin is required for transformation. Cancer Res. 2007; 67:7275–83. [PubMed: 17671196]
21. Chen YX, et al. The tumor suppressor menin regulates hematopoiesis and myeloid transformation by influencing Hox gene expression. Proc Natl Acad Sci U S A. 2006; 103:1018–23. [PubMed: 16415155]
22. Chandrasekharappa SC, et al. Positional cloning of the gene for multiple endocrine neoplasia-type 1. Science. 1997; 276:404–7. [PubMed: 9103196]
23. Marx SJ. Molecular genetics of multiple endocrine neoplasia types 1 and 2. Nat Rev Cancer. 2005; 5:367–75. [PubMed: 15864278]
24. Hughes CM, et al. Menin associates with a trithorax family histone methyltransferase complex and with the hoxc8 locus. Mol Cell. 2004; 13:587–97. [PubMed: 14992727]
25. Yokoyama A, et al. Leukemia proto-oncoprotein MLL forms a SET1-like histone methyltransferase complex with menin to regulate Hox gene expression. Mol Cell Biol. 2004; 24:5639–49. [PubMed: 15199122]
26. Grembecka J, Belcher AM, Hartley T, Cierpicki T. Molecular basis of the mixed lineage leukemia-menin interaction: implications for targeting mixed lineage leukemias. J Biol Chem. 2010; 285:40690–8. [PubMed: 20961854]
27. Mayer M, Meyer B. Group epitope mapping by saturation transfer difference NMR to identify segments of a ligand in direct contact with a protein receptor. J Am Chem Soc. 2001; 123:6108–17. [PubMed: 11414845]
28. Murai MJ, Chruszcz M, Reddy G, Grembecka J, Cierpicki T. Crystal structure of Menin reveals the binding site for mixed lineage Leukemia (MLL) protein. J Biol Chem. 2011
29. Mosmann T. Rapid colorimetric assay for cellular growth and survival: application to proliferation and cytotoxicity assays. J Immunol Methods. 1983; 65:55–63. [PubMed: 6606682]
30. Lavau C, Szilvassy SJ, Slany R, Cleary ML. Immortalization and leukemic transformation of a myelomonocytic precursor by retrovirally transduced HRX-ENL. EMBO J. 1997; 16:4226–37. [PubMed: 9250666]
31. Thiel AT, et al. MLL-AF9-induced leukemogenesis requires coexpression of the wild-type Mll allele. Cancer Cell. 2010; 17:148–59. [PubMed: 20159607]

32. Drabkin HA, et al. Quantitative HOX expression in chromosomally defined subsets of acute myelogenous leukemia. Leukemia. 2002; 16:186–95. [PubMed: 11840284]
33. Yokoyama A, Lin M, Naresh A, Kitabayashi I, Cleary ML. A higher-order complex containing AF4 and ENL family proteins with P-TEFb facilitates oncogenic and physiologic MLL-dependent transcription. Cancer Cell. 2010; 17:198–212. [PubMed: 20153263]
34. Thompson A, et al. Global down-regulation of HOX gene expression in PML-RARalpha + acute promyelocytic leukemia identified by small-array real-time PCR. Blood. 2003; 101:1558–65. [PubMed: 12560242]
35. Fiskus W, et al. Histone deacetylase inhibitors deplete enhancer of zeste 2 and associated polycomb repressive complex 2 proteins in human acute leukemia cells. Mol Cancer Ther. 2006; 5:3096–104. [PubMed: 17172412]
36. Golub TR, et al. Molecular classification of cancer: class discovery and class prediction by gene expression monitoring. Science. 1999; 286:531–7. [PubMed: 10521349]
37. Quentmeier H, et al. Expression of HOX genes in acute leukemia cell lines with and without MLL translocations. Leuk Lymphoma. 2004; 45:567–74. [PubMed: 15160920]
38. Thomas M, et al. Targeting MLL-AF4 with short interfering RNAs inhibits clonogenicity and engraftment of t(4;11)-positive human leukemic cells. Blood. 2005; 106:3559–66. [PubMed: 16046533]
39. Armstrong SA, et al. MLL translocations specify a distinct gene expression profile that distinguishes a unique leukemia. Nat Genet. 2002; 30:41–7. [PubMed: 11731795]
40. Milne TA, et al. Menin and MLL cooperatively regulate expression of cyclin-dependent kinase inhibitors. Proc Natl Acad Sci U S A. 2005; 102:749–54. [PubMed: 15640349]
41. Muntean AG, et al. The PAF complex synergizes with MLL fusion proteins at HOX loci to promote leukemogenesis. Cancer Cell. 2010; 17:609–21. [PubMed: 20541477]
42. Milne TA, et al. MLL associates specifically with a subset of transcriptionally active target genes. Proc Natl Acad Sci U S A. 2005; 102:14765–70. [PubMed: 16199523]

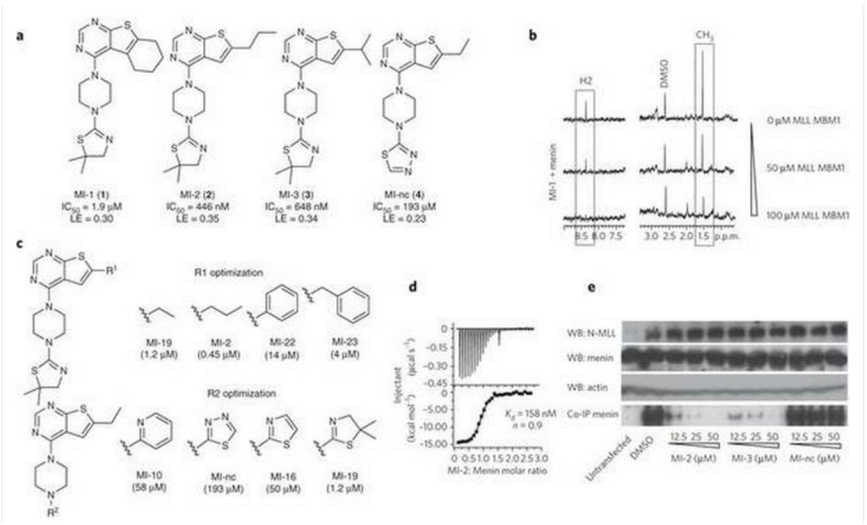

Figure 1. Characterization of the menin-MLL inhibitors

(a) Structures and IC_{50} values measured by FP for the inhibitors of the menin-MLL interaction, **MI-1**, **MI-2**, **MI-3** and **MI-nc.** LE (ligand efficiency) values were calculated according to the formula: LE=R*T*ln(IC_{50})/HA; where R is gas constant, T is temperature and HA is a number of non-hydrogen atoms in the compound. (**b**) NMR saturation transfer difference (STD) experiments. Top spectrum: 1D STD spectrum of **MI-1** (200 μM) with menin (5 μM). Boxes show STD effect for **MI-1** signals, corresponding to the aromatic proton from pyrimidine ring (H2) and two methyl groups at thiazoline ring (CH3). Middle and bottom spectra represent STD spectra for **MI-1** (200 μM) with menin (5 μM) and increasing concentrations of MLL MBM1 peptide (50 μM and 100 μM, respectively). (**c**) SAR for selected analogues of **MI-1** with different R1 and R2 substituents. (**d**) ITC experiment demonstrating direct binding of **MI-2** to menin with 1:1 stoichiometry. (**e**) Co-IP experiment in HEK293 cells transfected with Flag-MLL-AF9. **MI-nc** was used as a negative control. Untransfected cells serve as a control for endogenous expression of menin and lack of MLL-AF9 expression. WB, Western Blot; LE, ligand efficiency; ppm – parts per million; MBM1 – menin binding motif 1.

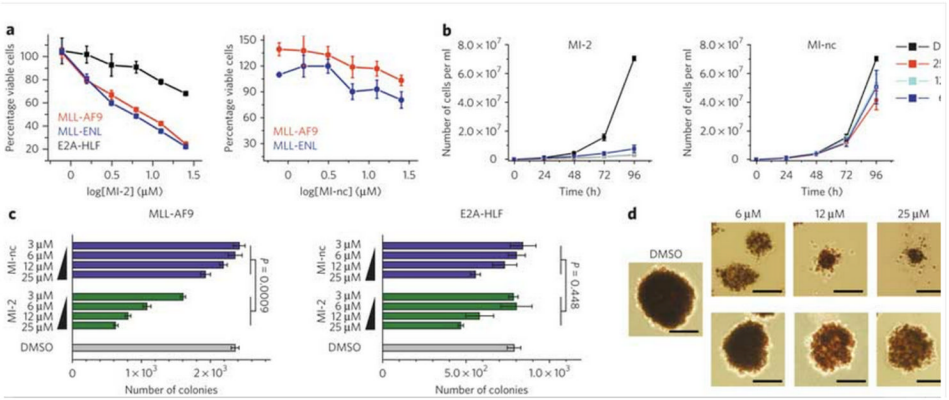

Figure 2. MI-2 induces growth arrest and inhibits transformation in MLL fusion-transduced bone marrow cells

(**a**) **MI-2** inhibits proliferation of mouse BMC transduced with MLL-AF9 or MLL-ENL but not E2A-HLF (left panel) as detected by MTT cell viability assay. **MI-nc** is a negative control (right panel). Data represent mean values for quadruplicates ± s.d. Experiments were performed three times. (**b**) Growth curves for **MI-2** (left panel) and **MI-nc** (right panel) treated MLL-AF9 transduced BMC grown in liquid culture. Data represent mean values for duplicate samples ± s.d. (**c**) Colony counts for methylcellulose colony assay performed with MLL-AF9 transduced BMC (left panel) and E2A-HLF transduced BMC (right panel) treated for 7 days with **MI-2** and **MI-nc.** Error bars indicate SD from duplicate experiments; two-way ANOVA analysis demonstrates statistical significance of the effect observed for **MI-2** as compared to **MI-nc** ($P<0.001$) in MLL-AF9 transduced BMC, and no significant difference between **MI-2** or **MI-nc** treated E2A-HLF transduced BMC ($P=0.448$). Experiments were performed three times. (**d**) Representative colonies shown for DMSO, **MI-2** and **MI-nc** treated MLL-AF9 transduced BMC plated on methylcellulose. Scale bars are 200 μm.

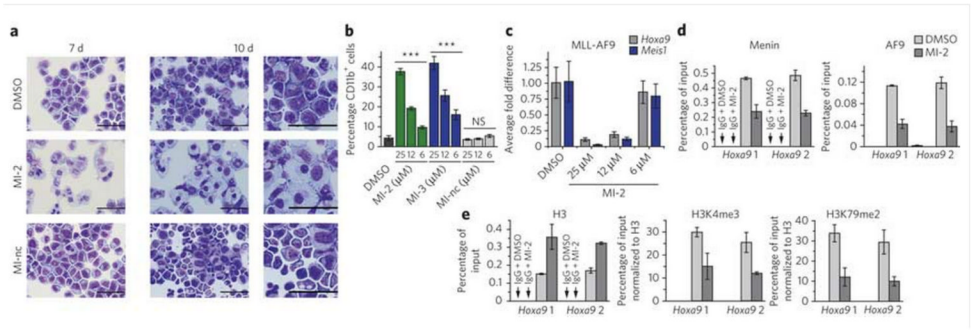

Figure 3. MI-2 induces hematopoietic differentiation and affects expression of MLL fusion protein target genes

(**a**) Wright-Giemsa stained cytospins on MLL-AF9 transformed BMC after 7 or 10 days of treatment with DMSO, **MI-2** (25 μM) and **MI-nc** (25 μM). Last column represents zoom for cells after 10 days of treatment. (**b**) Quantification of CD11b expression in MLL-AF9 transduced BMC treated for 7 days with the menin-MLL inhibitors as detected by flow cytometry. Data represent mean values for triplicates ± s.d. Statistical analysis was performed using one way ANOVA relative to DMSO treated control (*** indicates $P < 0.001$, ns – not significant). Experiment was performed three times. (**c**) Quantitative real-time PCR showing the expression of *Hoxa9* and *Meis1* in MLL-AF9 transduced BMC upon 6 days of treatment with **MI-2**. Expression of *Hoxa9* and *Meis1* was normalized to β-actin and referenced to DMSO treated cells. Data represent mean values for triplicates ± s.d. Experiment was performed three times. (**d, e**) ChIP experiments with antibodies against menin, AF9 and IgG (**d**), or H3, H3K4me3, H3K79me2 and IgG (**e**) in the MLL-AF9 transduced BMC after treatment with **MI-2** at 12.5 μM or DMSO. Binding was assessed at two sites (*Hoxa9* 1 and *Hoxa9* 2) in the promoter region. The signal for H3K4me3 and H3K79me2 was normalized relatively to H3 input. Data represent mean values for duplicate samples ± s.d. Experiment was performed two times.

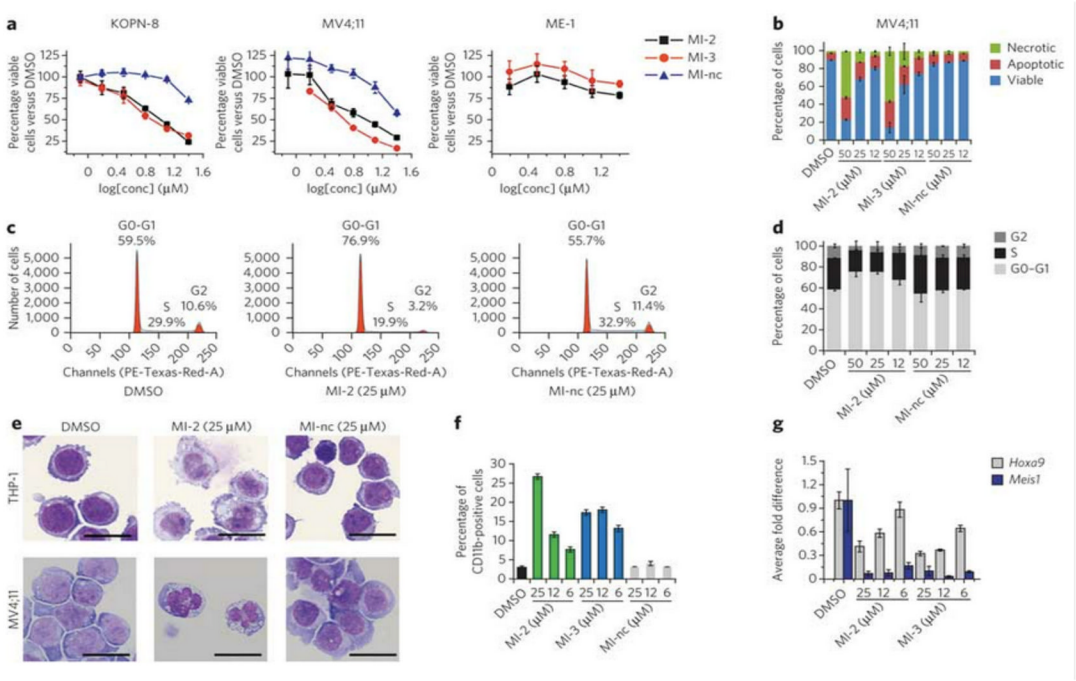

Figure 4. Effect of MI-2 and MI-3 in human MLL leukemia cells

(**a**) MTT cell viability assay in the MLL leukemia cells KOPN-8 and MV4;11 induced by **MI-2**, **MI-3** and **MI-nc** after 72h treatment. Non-MLL leukemia cell line ME-1 is shown for comparison. Data represent mean values for four samples ± s.d. Experiment was performed three times. (**b**) Apoptosis and cell death induced by **MI-2**, **MI-3** and **MI-nc** in MV4;11 cells as detected by flow cytometry using AnnexinV/propidium iodide (PI) staining. Data represent mean values for triplicates ± s.d. (**c**) Selected histograms from cell cycle analysis performed by FACS after PI staining in MV4;11 cells treated with DMSO, **MI-2** or **MI-nc.** (**d**) Dose-dependent effect of **MI-2** on cell cycle progression measured by FACS in MV4;11 cells after PI staining, with **MI-nc** as a negative control. Data represent mean values for triplicates ± s.d. (**e**) Wright-Giemsa stained cytospins on THP-1 and MV4;11 cells after 10 days of treatment with DMSO, **MI-2** or **MI-nc**. (**f**) Detection of CD11b expression in THP-1 cells assessed by flow cytometry after 6 days of treatment with **DMSO**, **MI-2** or **MI-nc**. Data represent mean values for triplicates ± s.d. (**g**) Expression of the *HOXA9* and *MEIS1* genes normalized to 18S rRNA determined by qRT-PCR in THP-1 cells treated for 6 days with **MI-2** and **MI-3**. Data represent mean values for duplicates ± s.d. Experiment was performed three times.